Ion-irradiation-induced preferential amorphization of Ge nanocrystals in silica

M. C. Ridgway*
Department of Electronic Materials Engineering, Research School of Physical Sciences and Engineering, Australian National University, Canberra, Australia

G. de M. Azevedo
Laboratório Nacional de Luz Síncrotron, Campinas, Brazil

R. G. Elliman, C. J. Glover, D. J. Llewellyn, R. Miller,† and W. Wesch‡
Department of Electronic Materials Engineering, Research School of Physical Sciences and Engineering, Australian National University, Canberra, Australia

G. J. Foran
Australian Nuclear Science and Technology Organisation, Menai, Australia

J. Hansen and A. Nylandsted-Larsen
Institute of Physics and Astronomy, University of Aarhus, Aarhus, Denmark
(Received 9 June 2004; revised manuscript received 8 November 2004; published 24 March 2005)

Extended x-ray absorption fine structure (EXAFS) measurements have been used to characterize the ion-irradiation-induced crystalline-to-amorphous phase transformation in Ge nanocrystals. The atomic-scale structure of Ge nanocrystals in a silica matrix is first shown to deviate from that of bulk crystalline material with an increase in both Gaussian and non-Gaussian forms of structural disorder. The magnitude of the disorder in the bond-length distribution is comparable to that of relaxed amorphous Ge. The amorphization of such nanocrystals is then demonstrated at an ion dose ~100 times less than that required for bulk crystalline material irradiated simultaneously. Specifically, Ge nanocrystals irradiated at −196 °C are rendered amorphous at ~0.01 displacements per atom. Finally, we show the atomic-scale structure of amorphized nanocrystals and bulk amorphous material is comparable. The rapid amorphization of Ge nanocrystals is potentially the result of several factors including (i) the preferential nucleation of the amorphous phase at the nanocrystal/matrix interface, (ii) the preirradiation, higher-energy structural state of the nanocrystals themselves, (iii) an enhanced vacancy concentration within the nanocrystals due to inhibited Frenkel pair recombination when Ge interstitials are recoiled into the matrix, and (iv) ion-beam mixing and the subsequent increase in nanocrystal impurity concentrations.

DOI: 10.1103/PhysRevB.71.094107 PACS number(s): 64.70.Nd, 61.10.Ht, 61.80.Jh, 61.48.+c

INTRODUCTION

The ion-irradiation-induced crystalline-to-amorphous phase transformation in bulk semiconductor substrates has been studied extensively and the relative influences of implant parameters such as ion mass, energy, dose, dose rate, and implant temperature are now well established.[1] Semiconductors in nanocrystalline form commonly exhibit differences in material properties relative to their bulk counterparts and only very recently have nanocrystals been subjected to ion irradiation.[2–5] For ion-irradiated Si nanocrystals in a silica matrix, measurements of the photoluminescence (PL) intensity and lifetime as functions of ion dose demonstrated the PL was rapidly quenched at ion doses insufficient for nanocrystal amorphization.[4,5] At higher ion doses, the amorphous nature of the nanocrystals was confirmed with transmission electron microscopy.[2,4,5] The critical ion dose required to render Si nanocrystals amorphous was significantly less than that determined previously for bulk crystalline substrates. In this report, the ion-irradiation-induced crystalline-to-amorphous phase transformation of Ge nanocrystals in a silica matrix is studied with extended x-ray absorption fine structure (EXAFS) measurements. As demonstrated previously, this synchrotron-radiation-based analytical technique is ideally suited for the study of both structural perturbations in nanocrystalline Ge (Refs. 6 and 7) and the crystalline-to-amorphous phase transformation in bulk Ge.[8] We characterize the phase transformation in Ge nanocrystals and, from measurements on bulk samples irradiated simultaneously, present a direct comparison of the ion-dose dependence of the amorphization process in a nanocrystalline and bulk semiconductor material. Thereafter, we establish the mechanisms responsible for the rapid amorphization of a semiconductor nanocrystal ensemble in a silica matrix.

EXPERIMENTAL

Amorphous silica (SiO_2) layers of thickness 2 μm were grown by wet thermal oxidation of (100) Si substrates. Samples were then implanted at a temperature of −196 °C with 2.0 MeV ^{74}Ge ions to an ion dose of $1\times10^{17}/cm^2$, yielding a peak Ge concentration of ~3 at. % at a depth of

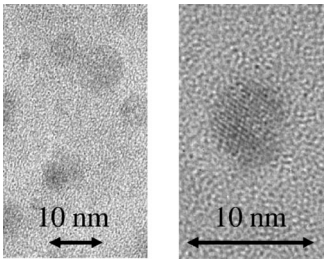

FIG. 1. Cross-sectional TEM micrographs of Ge nanocrystals in SiO_2.

$\sim 1\ \mu$m. To induce precipitation and nanocrystal growth, samples were subsequently annealed in flowing forming gas for 1 h at a temperature of 1100 °C. The resulting nanocrystal size distribution had a mean diameter of ~ 8 nm and a full width at half maximum of ~ 4 nm as determined with transmission electron microscopy. Figure 1 shows representative micrographs. The nanocrystals were clearly crystalline and electron diffraction confirmed they had the bulk (diamond) crystallographic structure.

Bulklike standards were prepared by depositing 250 nm of Ge by molecular beam epitaxy on both oxidized and nonoxidized (100) Si substrates yielding polycrystalline and epitaxially aligned single-crystalline layers, respectively. These samples were then coated with 1 μm of SiO_2, using plasma-enhanced chemical vapor deposition, yielding buried Ge layers at a depth comparable to that of the peak Ge concentration in the ion-implanted samples. During subsequent ion irradiation, the ion stopping powers over the Ge nanocrystal distribution and the deposited Ge layers were thus comparable.

Nanocrystalline, polycrystalline and single-crystalline samples were then irradiated simultaneously at a temperature of −196 °C with 5 MeV ^{28}Si ions as a function of ion dose. The projected range of such ions was $\sim 3\ \mu$m and the nuclear energy deposition over the extent of the Ge nanocrystal distribution and deposited Ge layers was approximately constant. Following ion irradiation, the SiO_2 surface layer over the single-crystalline samples was removed using dilute HF. The crystalline-to-amorphous phase transformation in bulk material was then characterized with Rutherford backscattering spectrometry combined with channeling (RBS/C) using 2 MeV ^{4}He ions and a scattering angle of 168°. Figure 2 shows representative RBS/C spectra as a function of Si ion dose. The critical ion dose for amorphization of bulk Ge was $\sim 2\times 10^{15}/\mathrm{cm}^2$ or ~ 1 displacement per atom (dpa).

Prior to the EXAFS measurements, the Si substrate below the ion-irradiated layers was removed using a combination of mechanical grinding and selective chemical etching (KOH in H_2O). The silica films of thickness 2 μm containing the irradiated nanocrystals were then stacked together for subsequent EXAFS analysis. The resulting increase in effective Ge areal density and the elimination of scattering from the Si substrate yielded a significant improvement in signal-to-noise ratio and enabled the high-resolution measurements presented below. The irradiated polycrystalline samples were processed in the same manner though the thickness of the Ge layer (250 nm) negated the need to stack such samples.

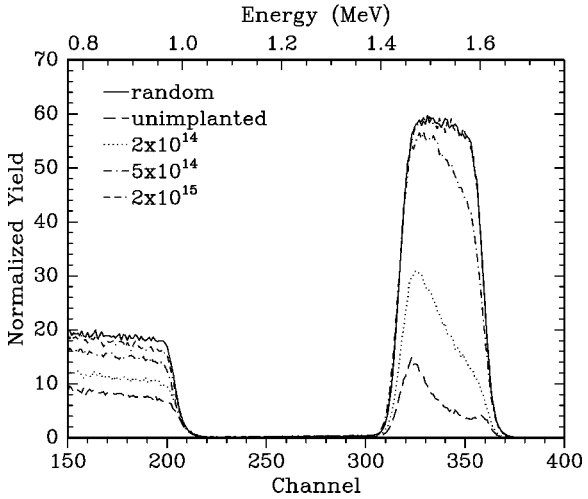

FIG. 2. RBS/C spectra of single-crystalline Ge (on a Si substrate) as a function of Si ion dose (in units of ions/cm^2).

Fluorescence-mode EXAFS measurements were performed at a temperature of 15 K at beam lines 20-B of the Photon Factory, Japan, and 7-3 of the Stanford Synchrotron Radiation Laboratory, USA. Fluorescence spectra were recorded with a multielement solid-state Ge detector, at the Ge *K* edge (11.103 keV), with the Si (111) monochromator detuned by 50% for harmonic rejection. Data were analyzed following the procedure described in Ref. 7. EXAFS spectra were isolated from the raw absorption by background subtraction and subsequent splining using SPLINE.[9] Structural parameters were then determined using IFEFFIT (Ref. 10) with photoelectron momentum (k) and non-phase-corrected radial distance (r) ranges of 4–17.1 Å^{-1} and 1.6–2.6 Å, respectively. Phases and amplitudes were calculated *ab initio* with FEFF8.0.[11] The amplitude reduction factor ($S_0{}^2$) and threshold energy (E_0) were determined from the polycrystalline standard and held constant thereafter. A given data set was fitted simultaneously with multiple k weightings of 1–4.

RESULTS AND DISCUSSION

Figure 3(a) displays k^3-weighted EXAFS spectra as a function of photoelectron momentum comparing polycrystalline and nanocrystalline samples *prior* to ion irradiation. The data quality of the spectra is readily apparent. The corresponding Fourier transforms are shown in Fig. 3(b) as a function of non-phase-corrected radial distance. Table I compares the three moments of the nearest-neighbor shell for nanocrystalline, polycrystalline, and bulk amorphous Ge samples, the latter in a thermally relaxed, minimum-energy state.[12] (As formed, the structural parameters of bulk amorphous Ge fabricated by ion implantation are ion-dose dependent.[13] Annealing for 1 hr at 200 °C yields a less-disordered amorphous structure common to all samples and independent of the implant conditions.[12]) The bondlengths for the nanocrystalline and polycrystalline samples are equal yet the former exhibits a greater Debye-Waller factor and nonzero third moment (the latter demonstrating the presence

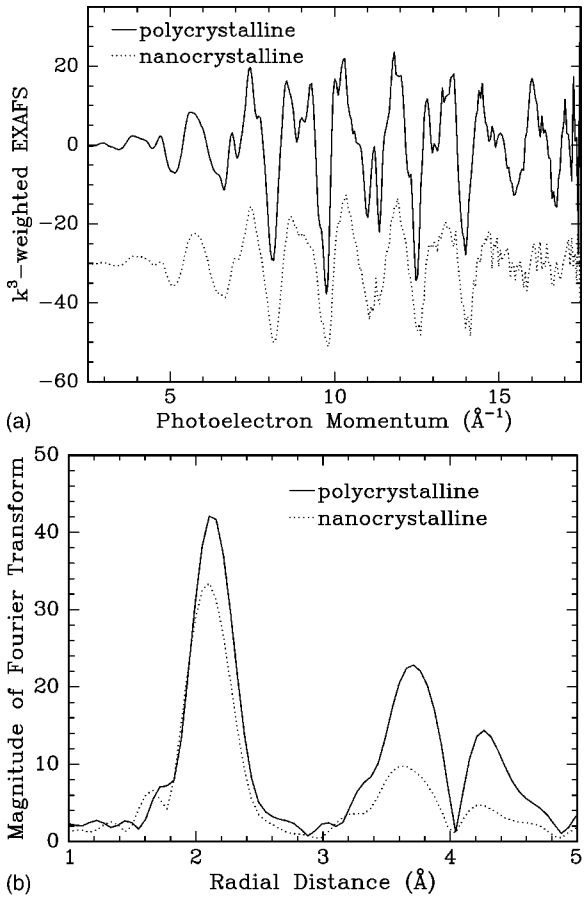

FIG. 3. (a) k^3-weighted EXAFS spectra as a function of photoelectron momentum comparing bulk polycrystalline and nanocrystalline samples prior to ion irradiation and (b) corresponding Fourier-transformed spectra as a function of non-phase-corrected radial distance.

of non-Gaussian static disorder). Evidently, disorder in the bond-length distribution of the nanocrystalline sample is comparable to that of relaxed amorphous material. The greater third moment of the former is the result of bonding distortions at or near the nanocrystal/matrix interface. In Fig. 3(b), structural disorder (in both the bond-length and bond-angle distributions) is manifested as the reduction in magnitude of the scattering contributions from the three nearest-neighbor shells. Finally, the slightly reduced coordination number of the nanocrystalline sample relative to polycrystalline (and relaxed amorphous) material is, as we calculated elsewhere,[7] a finite-size effect resulting from undercoordinated atoms at the nanocrystal/matrix interface. Such finite-size effects also reduce the magnitude of the Fourier-transformed spectrum but to a much lesser extent than structural disorder.

Figure 3(b) and Table I demonstrate the atomic-scale structure of the nanocrystalline sample is perturbed relative to that of polycrystalline material. Equivalently, the free energy of the nanocrystalline state exceeds that of the polycrystalline state. The causes of such perturbations have been discussed elsewhere[6] and include strain from bonding distortions at or near the nanocrystal/matrix interface. Given that EXAFS measurements represent the superposition of all Ge environments, the spatial extent of the structural perturbations cannot be readily determined from the single spectrum shown herein. Measurements as a function of nanocrystal size are in progress[14] to identify whether the perturbations are confined to the nanocrystal/matrix interface or are distributed homogeneously throughout the nanocrystal.

Figures 4(a) and 4(b) show Fourier transforms of k^3-weighted EXAFS spectra as a function of non-phase-corrected radial distance for ion-irradiated polycrystalline and nanocrystalline samples, respectively. In the former, ion irradiation yields a progressive decrease in amplitude of the scattering contributions from the three nearest-neighbor shells resulting from the loss of medium-range order. For a Si ion dose of $2\times10^{15}/\mathrm{cm}^2$, no scattering contributions from beyond the first shell are apparent consistent with complete amorphization. The short-range order characteristic of (poly)crystalline material was retained in the amorphous sample with each Ge atom bonded to four other Ge atoms at $r=\sim2.1$ Å. As above, the decrease in amplitude is the result of the increase in Debye-Waller factor or equivalently structural disorder. Note the critical ion doses for amorphization determined by RBS/C with single-crystalline samples (Fig. 2) and by EXAFS with polycrystalline samples (Fig. 4) were equal.

Striking differences in ion-dose dependence are apparent upon comparison with Fig. 4(b) for the nanocrystalline samples. (Note the dose ranges differ by a factor of 10 between the two figures.) The latter are evidently much more sensitive to ion irradiation than polycrystalline material. The scattering contributions beyond the first shell are effectively eliminated at an ion dose of $2\times10^{13}/\mathrm{cm}^2$ or ~0.01 dpa, ~100 times less than that required to amorphize polycrystalline material. (For a nanocrystal of diameter 8 nm, this equates to the gross ion-irradiation-induced displacement of ~120 atoms.) As above, the absence of scattering contributions from beyond the first shell is consistent with complete amorphization.

TABLE I. Structural parameters of polycrystalline, nanocrystalline, and relaxed amorphous Ge samples.

First shell	Coordination number (atoms)	Bondlength (Å)	Debye-Waller factor ($Å^2$)	Third cumulant ($Å^3$)
Polycrystalline Ge	4 (fixed)	2.449 ± 0.002	$(2.5\pm0.2)\times10^{-3}$	nil (fixed)
Nanocrystalline Ge	3.81 ± 0.20	2.450 ± 0.003	$(3.2\pm0.2)\times10^{-3}$	$(7.13\pm3.55)\times10^{-5}$
Relaxed amorphous Ge	3.97 ± 0.14	2.460 ± 0.002	$(3.1\pm0.3)\times10^{-3}$	$(2.30\pm0.20)\times10^{-5}$

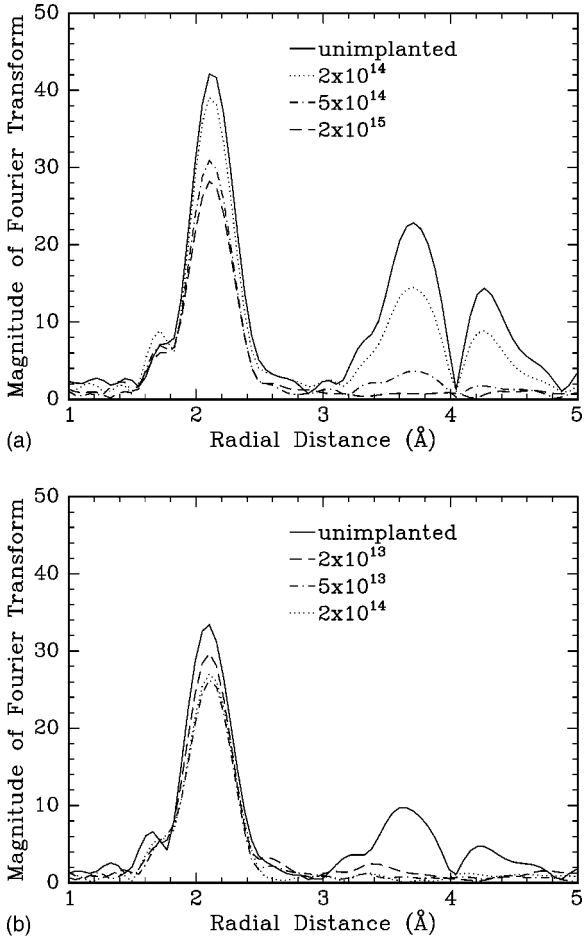

FIG. 4. Fourier-transformed k^3-weighted EXAFS spectra as a function of non-phase-corrected radial distance comparing (a) polycrystalline and (b) nanocrystalline samples following Si ion irradiation (in units of ions/cm^2).

Figure 5 compares the ion-dose dependence of one structural parameter—the Debye-Waller factor of the nearest-neighbor shell—for polycrystalline and nanocrystalline Ge samples. In the former, the crystalline-to-amorphous phase transformation is manifested by the gradual increase in Debye-Waller factor (or equivalently structural disorder) from the crystalline to amorphous values consistent with our previous reports for bulk Ge.[8] In contrast, the Debye-Waller factor of the nanocrystalline sample is effectively saturated at the amorphous value for the lowest ion dose examined.

Figure 6 shows the reconstructed interatomic distance distributions, before and after ion irradiation, for the polycrystalline and nanocrystalline samples. Prior to ion irradiation, the structural differences between the two samples are readily apparent as discussed previously. In the nanocrystalline-sample spectrum, the greater full-width-at-half-maximum results from the greater extent of static, Gaussian disorder while the asymmetry results from the presence of static, non-Gaussian disorder. Following amorphization, the spectra (and thus the structural parameters) for the polycrystalline and nanocrystalline samples are comparable and consistent with our previous reports for bulk amorphous Ge.[13] We now consider potential causes of the rapid amorphization of Ge nanocrystals.

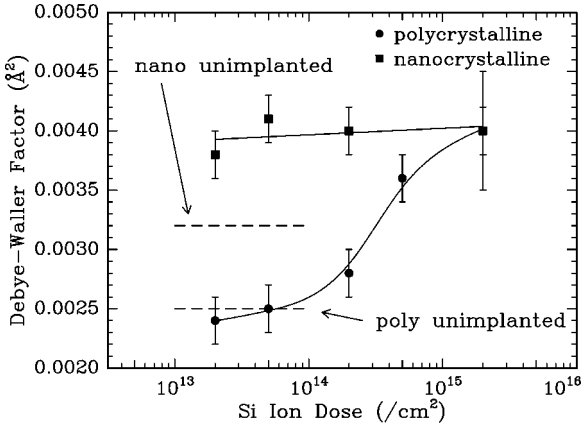

FIG. 5. Debye-Waller factor as a function of Si ion dose comparing polycrystalline and nanocrystalline samples.

Preferential nucleation of the amorphous phase at the nanocrystal/matrix interface. As previously noted by others,[4,5] under the appropriate conditions the surface of a Si substrate can be amorphized more readily than the bulk despite a greater nuclear energy deposition in the latter. The difference in mobility of (irradiation-induced) interstitials and vacancies causes the substrate surface to act as a superior sink for the more-mobile interstitials. In the immediate subsurface region, the vacancy concentration is thus increased yielding the observed enhanced nucleation of the amorphous phase. For the implant conditions listed above, *no* indication of preferential amorphization at the single-crystalline-Ge/SiO_2 interface was observed in the bulk standard with RBS/C (Fig. 2). However, given the much enhanced surface-area-to-volume ratio for a nanocrystal, the potential for preferential amorphization at (or immediately below) the nanocrystal/matrix interface is increased and the ion dose required for amorphization of the nanocrystal ensemble potentially decreased.

The pre-irradiation, higher-energy structural state of the nanocrystals. The structural parameters presented in Table I demonstrated that Ge nanocrystals were structurally perturbed relative to polycrystalline material *prior* to ion irradiation. The extent of disorder in the nanocrystal bond-length

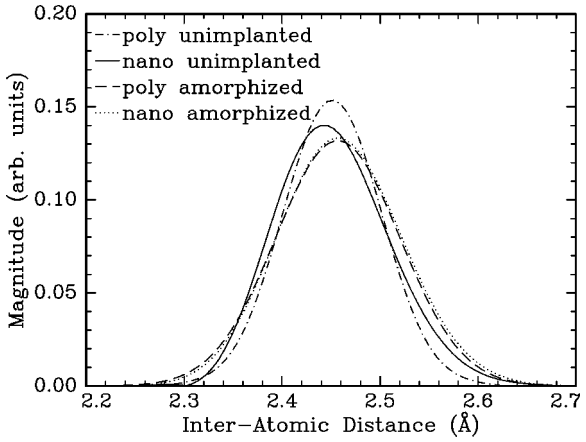

FIG. 6. Interatomic distance distributions, before and after ion irradiation, comparing polycrystalline and nanocrystalline samples.

distribution was comparable to that of relaxed amorphous material. Given irradiation yields an ion-dose-dependent increase in free energy per atom, increasing from the unimplanted, crystalline value to that of amorphous material, the higher-energy structural state of the nanocrystal *prior* to ion irradiation potentially decreases the ion dose required for amorphization of the nanocrystal ensemble.

Enhanced vacancy concentration within the nanocrystals. The nanocrystal vacancy concentration can be further enhanced when irradiation-induced interstitials are recoiled beyond the nanocrystal bounds. SRIM simulations[15] of a SiO_2 (1 μm)/Ge (8 nm)/SiO_2 (substrate) structure irradiated as above show the average recoil energy of a displaced Ge atom is $\sim$50 eV. Displacement collisions within $\sim$1 nm of the nanocrystal/matrix interface are thus capable of recoiling Ge atoms into the matrix, inhibiting Frenkel pair recombination. For a nanocrystal of 8 nm diameter, $>$50% of the atoms reside within 1 nm of the nanocrystal/matrix interface. Furthermore, the spherical nature of the nanocrystal increases the significance of this factor relative to SRIM simulations for a planar structure. This additional increase in the nanocrystal vacancy concentration potentially further decreases the ion dose required for amorphization of the nanocrystal ensemble.

Ion-beam mixing. Recoiling of both nanocrystal and matrix atoms will yield ion-beam mixing at and near the nanocrystal/matrix interface. SRIM simulations[15] as above demonstrated that for an ion dose of $2\times10^{13}/\mathrm{cm}^2$, the recoiled O concentration immediately below the nanocrystal/matrix interface was $\sim$0.05 at. %, decreasing by a factor of 100 in the midst of the nanocrystal. The presence of O impurities could aid in stabilizing the amorphous phase and potentially further decrease the ion dose required for amorphization.

Quantification of the relative contributions of the four factors described above is not readily achievable. Such a determination is impeded by a common size dependence—though we anticipate the ion dose required for amorphization will decrease as the nanocrystal size decreases, the influence of each of the four factors necessarily increases as the surface-area-to-volume ratio increases. Others[4,5] have attributed the rapid amorphization of Si nanocrystals to preferential nucleation of the amorphous phase at the nanocrystal/matrix interface though no evidence of such an effect was observed herein with bulk standards. Furthermore, our simulations of the recoiled nanocrystal and matrix atom distributions suggest it is improbable that the $\sim$100-fold decrease in the ion dose required for amorphization is the sole result of mixing. We have however measured and compared the atomic-scale structural parameters of both the nanocrystal ensemble and bulk standards throughout the course of the phase transformation. Structural disorder in the nanocrystal bond-length distribution *prior* to ion irradiation was similar to of relaxed amorphous material. We now speculate that such structural perturbations render semiconductor nanocrystals significantly more prone to amorphization by ion irradiation.

CONCLUSIONS

In summary, the results presented above demonstrate (i) prior to ion irradiation, Ge nanocrystals exhibit subtle structural perturbations relative to polycrystalline material, (ii) Ge nanocrystals are rendered amorphous at an ion dose $\sim$100 times less than that required for polycrystalline material, and (iii) following amorphization, Ge nanocrystals and polycrystalline material have a common (amorphous) structure. The factors that can reduce the irradiation resistance of Ge nanocrystals include: (i) preferential nucleation of the amorphous phase at the nanocrystal/matrix interface, (ii) the higher-energy structural state of the nanocrystals prior to ion irradiation, (iii) an enhanced vacancy concentration resulting from the recoiling of interstitials beyond the nanocrystal bounds, and (iv) ion-beam mixing and the introduction of impurities. Combining a comparison with bulk standards and simulations of the extent of ion-beam mixing, we now speculate that semiconductor nanocrystals are more easily amorphized than bulk material due to their higher-energy structural state prior to ion irradiation.

ACKNOWLEDGMENTS

M.C.R., G.M.A., C.J.G., W.W., and G.J.F. were supported by the Australian Synchrotron Research Program and/or the Access to Major Research Facilities Program, both of which are funded by the Commonwealth of Australia. M.C.R. also thanks the Australian Research Council for support. W.W. thanks the Australian National University (ANU), the Friedrich Schiller University and the Thuringian Ministry of Science, Research and Art for financial support.

*Email address: mcr109@rsphysse.anu.edu.au
†Current address: Institut fur Physik, University of Augsburg, Augsburg, Germany.
‡Permanent address: Institut fur Festkorperphysik, Friedrich-Schiller University, Jena, Germany.

[1] For example, see P. J. Schultz, C. Jagadish, M. C. Ridgway, R. G. Elliman, and J. S. Williams, Phys. Rev. B **44**, 9118 (1991).
[2] G. A. Kachurin, M.-O. Ruault, A. K. Gutakovsky, O. Kaitasov, S. G. Yanovskaya, K. S. Zhuravlev, and H. Bernas, Nucl. Instrum. Methods Phys. Res. B **147**, 356 (1999).
[3] S. Cheylan, N. Langford, and R. G. Elliman, Nucl. Instrum. Methods Phys. Res. B **166–167**, 851 (2000).
[4] D. Pacifici, E. C. Moreira, G. Franzo, V. Martorino, F. Priolo, and F. Iacona, Phys. Rev. B **65**, 144109 (2002).
[5] D. Pacifici, G. Franzo, F. Iacona, and F. Priolo, Physica E (Amsterdam) **16**, 404 (2003).
[6] A. Cheung, G. de M. Azevedo, C. J. Glover, D. J. Llewellyn, R. G. Elliman, G. J. Foran, and M. C. Ridgway, Appl. Phys. Lett. **84**, 278 (2004).
[7] M. C. Ridgway, G. de M. Azevedo, C. J. Glover, R. G. Elliman, D. J. Llewellyn, A. Cheung, B. Johannessen, D. A. Brett, and G. J. Foran, Nucl. Instrum. Methods Phys. Res. B **218**, 421 (2004).

[8] C. J. Glover, M. C. Ridgway, A. P. Byrne, K. M. Yu, G. J. Foran, C. Clerc, J. L. Hansen, and A. Nylandsted Larsen, Nucl. Instrum. Methods Phys. Res. B **161–163**, 1033 (2000).
[9] P. J. Ellis and H. Freeman, J. Synchrotron Radiat. **2**, 190 (1995).
[10] M. Newville, J. Synchrotron Radiat. **8**, 322 (2001).
[11] A. L. Akudinov, B. Ravel, J. J. Rehr, and S. D. Conradson, Phys. Rev. B **58**, 7565 (1998).
[12] C. J. Glover, M. C. Ridgway, K. M. Yu, G. J. Foran, I. D. Desnica-Frankovic, C. Clerc, J. L. Hansen, and A. Nylandsted Larsen, Phys. Rev. B **63**, 073204 (2001).
[13] M. C. Ridgway, C. J. Glover, K. M. Yu, G. J. Foran, C. Clerc, J. L. Hansen, and A. Nylandsted Larsen, Phys. Rev. B **61**, 12 586 (2000).
[14] C. J. Glover (unpublished).
[15] J. F. Ziegler, URL http://srim.org